

# Residual Strength Prediction Model for Corroded Oil Tube based on FEM and Artificial Neural Network

M. Y. Xia\*, H. Zhang

*College of Mechanical and Transportation Engineering, China University of Petroleum–Beijing, Beijing 102249, China*

[\\*xiamengying322@163.com](mailto:*xiamengying322@163.com)

## Abstract

Corroded oil tubes are prone to failure under complicated service load. In this study, finite element models of oil tubes with two typical shape of corrosion defects, e.g. elliptical corrosion pits and the axial groove defects, under the service loads were established. Based on the numerical model, parametric analysis were conducted to investigate the effects of corrosion defect position, defect depth, defect width and defect length on tube's residual strength. Finally, based on derived numerical results, a BP artificial neural network (ANN) was employed to predict the residual strength of corroded oil tube. Results show that, when the corrosion location depth is shallow, the failure of oil tubes are mainly caused by the axial force. When the corrosion location depth is deep, the failure is mainly caused by the internal pressure. With increase of the depth in well of the corrosion defect, the max von Mises stress in the tube decreases first and then increases. The corrosion defect depth has a great influence on tube's max von Mises stress. While the corrosion width and length have small influence on tube's max von Mises stress. By validation with numerical results, the proposed BP ANN based residual strength prediction model was accurate and efficiency. This proposed method can be referred in the assessment of oil tubes with corrosion defects.

**Keywords:** corrosion defects, oil tube, finite element method, residual strength, artificial neural network

## Introduction

Oil tubes play a very important role in oil field development. The complicated working environments make it vulnerable to external loads. Corrosion is one main threat for these oil tubes. Fig.1 shows some corroded oil tubes in engineering practice. It is obvious that, metal losses in the tube's inner and outer surface. Thus conducting failure analysis or safety assessment of corroded oil tubes has important practical significance.

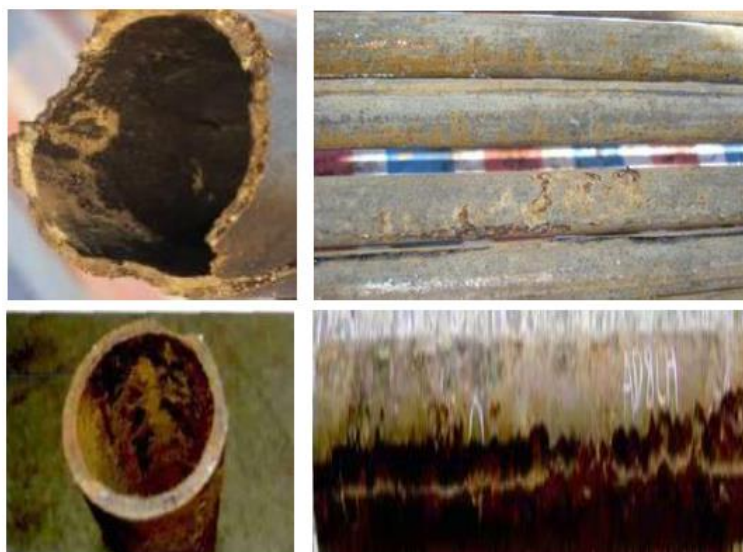


**Fig.1** Corroded oil tubes

In recent years, there are a series of available literatures on strength analysis of oil pipelines and tubes with corrosion defects, especially pipelines. Batte et al. proposed a regression based residual strength prediction model for corroded oil pipes [1]. Choi et al. and Chen et al. also obtained some simple formulas for limit pressure of pipes with corrosion defects by numerical analysis [2,3]. Shuai et al. proposed an improved limit pressure prediction model for both low strength and high strength steel pipes [4]. Stephens et al., Leis et al., Fekete et al. discussed the effects of geometrical parameters of corrosion defects on pipe's residual strength [5, 6, 7]. Xiao et al. and Peng et al. compared the different assessment methods for corroded pipes adopted by various standards or guidelines [8, 9]. Zhou et al. discussed the failure criterion of corroded oil tube by experimental and numerical investigation [10]. Hu et al. established a finite element model for stress analysis of riser with narrow and long defects, and based on the numerical model, reliability analysis was also conducted [11]. Liu et al. investigated the failure modes of corroded N80 oil tube under different load conditions [12]. Xia et al. conducted parametric analysis on the residual strength of N80 oil tube with different types of corrosion defect.

Although many researches have been done, few of them focused on the accurate residual strength prediction of corroded oil tube subjected to service loads, which is of great importance for engineering practice. To fill this gap, based on finite element method, a stress analysis numerical model for corroded oil tube subjected to service load was established by general finite element software package ANSYS. Two common corrosion defect types were considered in the investigation. A parametric analysis was performed to

derive the quantitative relationship between the influence factors and the max von Mises in the tube. Finally, an artificial neural network based prediction model was proposed for predicting the residual strength of corroded oil tube.

## Service load of oil tube

Under service condition, the oil tube is under complicated load condition [12]. In the vertical direction, it is under the gravity load and other kinds of load. In the circumferential direction, it is under internal pressure load. In some special cases, there will be additional bending load on the tube, which is not considered in this study.

For the applied vertical load on the tube, it is composed of the gravity load induced by the tube  $\sigma_1$ , the buoyancy force induced by the well fluid  $\sigma_2$ , the gravity load induced by the fluid  $\sigma_3$ , the friction load between the plunger and bush  $\sigma_4$ , the friction load between the pumping rod and the tube  $\sigma_5$  [10]. So the max axial load in the tube can be obtained as follow:

$$\sigma = \sigma_1 - \sigma_2 + \sigma_3 + \sigma_4 + \sigma_5 \quad (1)$$

For the internal pressure, it can be easily derived as:

$$P = \rho_0 gh + \sigma_0 \quad (2)$$

Where,  $h$  is the depth position of the defect in the tube,  $\rho_0$  is the density of the oil,  $g$  is the gravity acceleration,  $\sigma_0$  is the pressure at the well ahead.

## Numerical model

### Material properties

In the numerical model, true stress–strain of P110 steel was adopted in the numerical analysis. The multi–linear isotropic hardening model in ANSYS was utilized simulating this relationship. And according to API Specification 5CT, Specification for Casing and Tubing [15], typical material parameters for P110 steel are as follows. The Young's modulus  $E$  is 207GPa, the yield strength is 758MPa, the ultimate strength is 862MPa, the Possion ratio is 0.3.

### Finite element model

For oil tube corrosion defects, it has three main geometrical parameters, the corrosion depth  $d$ , the corrosion length  $L$ , the corrosion width  $W$ , as shown in Fig.2.

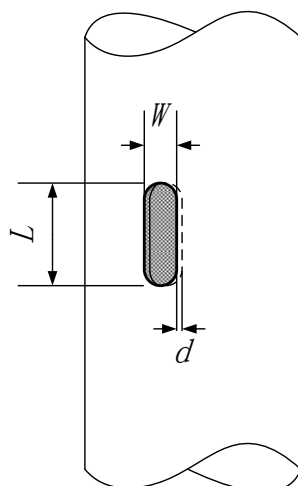


**Fig.2** Geometrical parameters of corrosion defect

For the model is symmetric, only one fourth of the tube need to be modelled in numerical analysis. In the numerical model, 20 node continuum solid element SOLID 186 was adopted to simulate the pipe. In the corrosion area, a fine mesh was used. In the radial direction, the tube was divided into four elements. The mesh details of the finite element model was shown in Fig. 3.

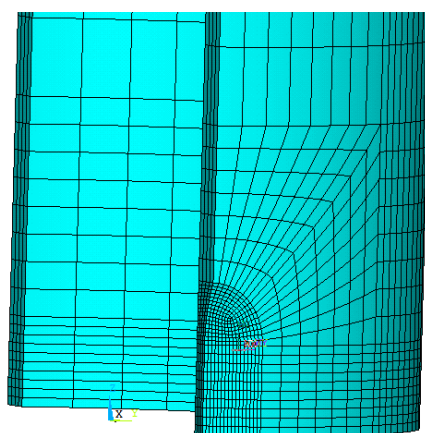


**Fig.3** Finite element model for corroded tube

## Model validation

For oil tube, rupture will occur when the von-Mises stress in the structure reaches the ultimate strength of the steel. This failure mechanism is similar for both oil tubes and pipelines. Thus in this section full scale experimental results for burst test of high strength pipelines were used to validate the accuracy of the presented model. Parameters of the

experiment specimens were listed in Table 1. The finite model was modified geometrically to conduct these analysis, and results were compared with the experimental and previous numerical results, as illustrated in Fig.4. It can be found that, results obtained by proposed finite element model agrees well with the other results, which proves this numerical model is reliable.

Table 1 Parameters for experiment corroded pipes

| No. | Pipe diameter/mm | Wall thickness/mm | Defect length /mm | Defect depth/mm |
|-----|------------------|-------------------|-------------------|-----------------|
| 1   | 1219             | 19.89             | 606               | 15.4            |
| 2   | 1219             | 19.89             | 606               | 7.4             |
| 3   | 1219             | 19.89             | 608               | 1.8             |
| 4   | 1219             | 13.79             | 588               | 10.8            |
| 5   | 1219             | 13.79             | 589               | 5.4             |
| 6   | 1219             | 13.79             | 586               | 1.5             |

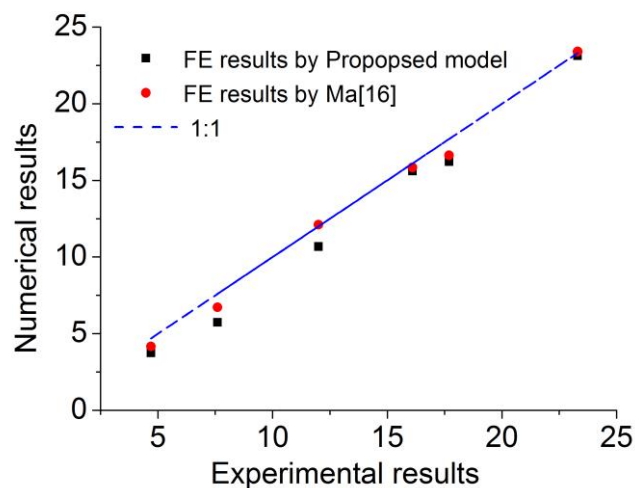


**Fig.4** Comparison results of proposed numerical model with previous experimental and numerical results

## Parametric analysis

In this section, parametric analysis was performed using the established numerical model to investigate the trends of the max von Mises stress  $\sigma_{max}$  with the influence factors. In this study, Typical P110 oil tube used in the Tahe oil field in China was considered. Thus the service load was calculated by the field data. Key parameters are as followed: the total depth of the well is 4500m, the density of completion fluids in the well is 973kg/m<sup>3</sup>, the viscosity of completion fluids in the well is 0.025Pa s, the pressure of the well head is 3.4MPa. In numerical analysis, the axial load and internal pressure in the tube are linear with the depth position of the corrosion defect in the tube.

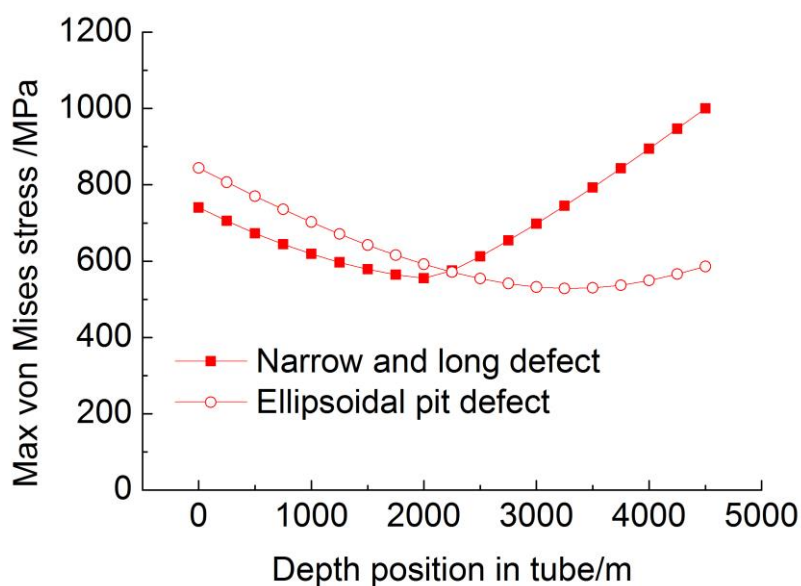
### Effects of load conditions

As mentioned above, with the increase of the depth position of the defect in tube  $h$ , the axial load in the tube decreases linearly, while the internal pressure increases linearly. In this section, two typical shapes of corrosion were considered to investigate the relationship of max von Mises stress in the tube  $\sigma_{max}$  with the depth position of defect in tube  $h$ . The first kind of corrosion defect is ellipsoidal pit defect, its geometrical parameters are listed as follows:  $L=20\text{mm}$ ,  $W=16\text{mm}$ ,  $d=4\text{mm}$ . another kind of corrosion defect is the narrow and long defect, its geometrical parameters are also listed as follows:  $L=60\text{mm}$ ,  $W=16\text{mm}$ ,  $d=4\text{mm}$ .

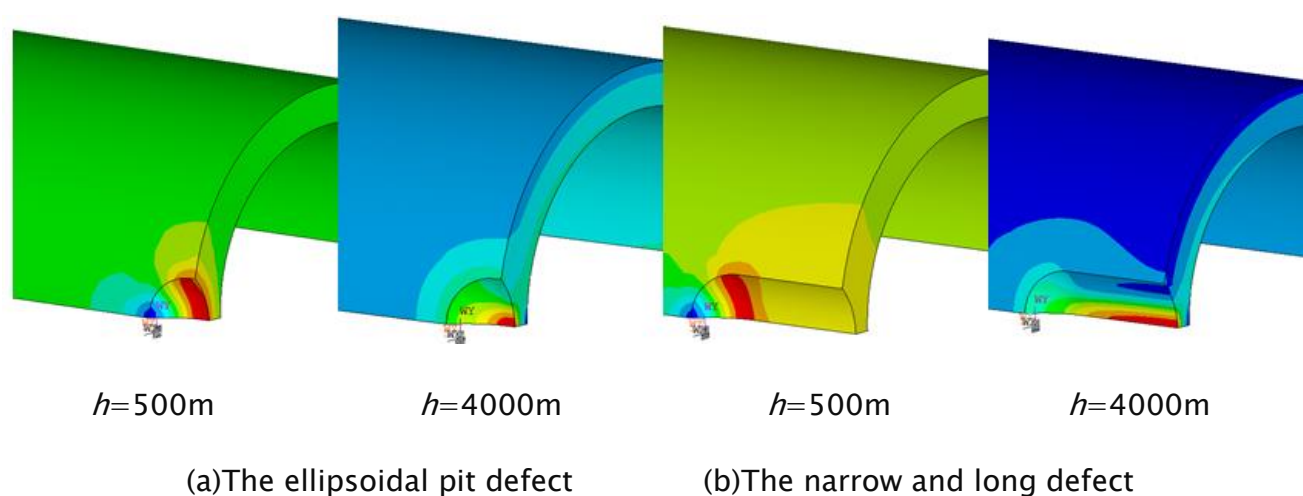
Fig. 5 shows trends of the max von mises stress  $\sigma_{max}$  with the depth position in the tube  $h$ . It can derived that, for both kinds of defects,  $\sigma_{max}$  increases with  $h$  first, and then decreases. By comparing the two curves, it can be found that, when  $h<2250\text{m}$ , the max stress of tube with ellipsoidal pit defect is larger than that with narrow and long defect.

Fig. 6 illustrates the detailed von Mises contours of the defect areas at different depth positions in tube for both types of defect. when  $h=500\text{m}$ , the max von Mises stresses concentrated at the axial central line and axial end of the defect area for ellipsoidal pit defect and narrow and long defect, respectively. While, when  $h=4000\text{m}$ , the max von Mises stresses concentrated at the circumferential central line for both types of defect. Thus if  $h$  is small, tube may rupture in axial direction, and if  $h$  is large enough, the tube may rupture in circumferential direction. The two failure phenomenon in engineering practice were shown in Fig. 7.





**Fig.5** Trends of the max von Mises stress with the depth position of the defect in tube



**Fig.6** The von Mises stress contours of defect areas at various depth positions in tube



(a) Axial rupture (b) Circumferential rupture

**Fig.7** Failure tubes with axial and circumferential rupture

### Effects of defect depth

The defect depth was described by the ratio of the defect depth with tube wall thickness in this study. The corrosion defect was set to be 4000m depth in well, thus the axial load was 148.65 MPa and the internal pressure was 41.54MPa.

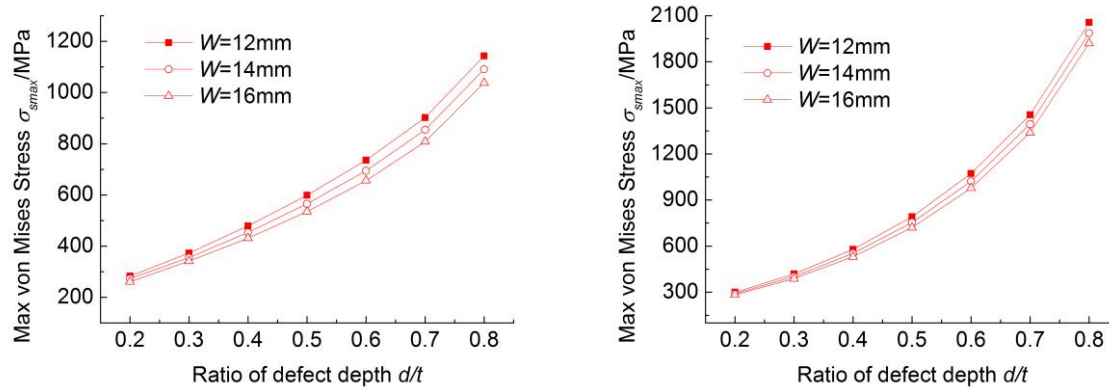
Fig. 8 illustrates the trends of the maximum von Mises stress with the defect depth for two different shape defects. Obviously, with increases of the defect depth, the maximum von Mises stress increases. And it increases faster with a larger defect depth. This phenomenon is similar for defects with different width. For the ellipsoidal pit defect, the maximum stress became larger than the yield strength of tube, when  $d/t=0.65$ . For the narrow and long defect, the maximum stress became larger than the yield strength of tube, when  $d/t=0.5$ .

Von Mises contours of the two defects with different defect depth were shown in Fig. 9. It can be obtained that, the stress distribution is similar for the two defects. And with increase of the defect depth, stress concentration become more severe in central area of the defect.

### Effects of defect width

Fig. 10 illustrates the relationship of the max von Mises stress with the defect width for two types of corrosion defect. The trends of max stress with defect width are similar for the two kinds of defects. When the depth of defect  $d/t$  is small, max von Mises stress  $\sigma_{\max}$  have very small variations with the increase of defect width. When  $d/t$  is larger,  $\sigma_{\max}$  decreases with the increase of the defect width. The main reason of this phenomenon is that, with the increase of defect width stress concentration can be reduced to some extent.

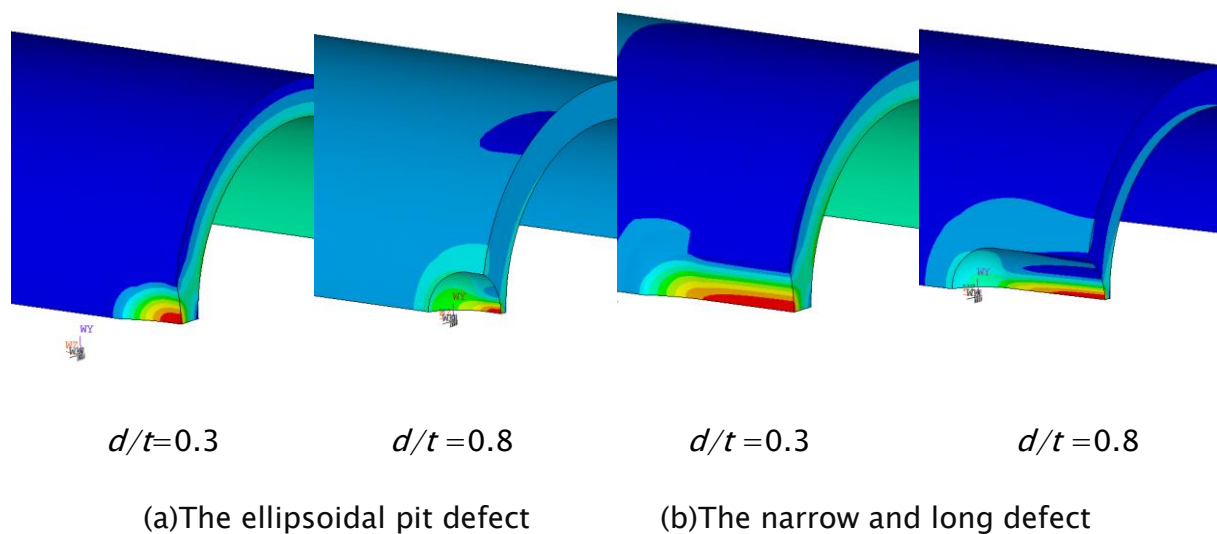




(a) The ellipsoidal pit defect

(b) The narrow and long defect

**Fig.8** Trends of the max von Mises stress with the depth of defect

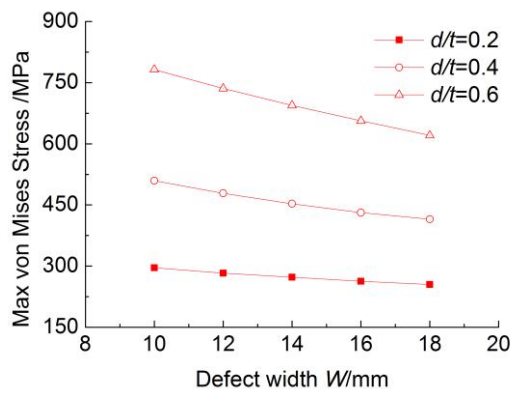


(a)The ellipsoidal pit defect

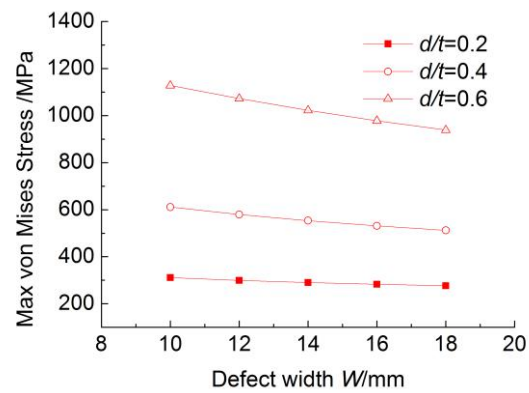
(b)The narrow and long defect

**Fig.9** The von Mises stress contours of defect areas with different defect depth

The von Mises stress contours for tubes with different defect width were also plotted in Fig. 11. For the ellipsoidal pit defect, with increase of the defect width, the max von Mises stress position transferred from the circumferential central line to the central defect area. For the narrow and long type defect, the von Mises stress distribution has no obvious difference, when the defect width increases.

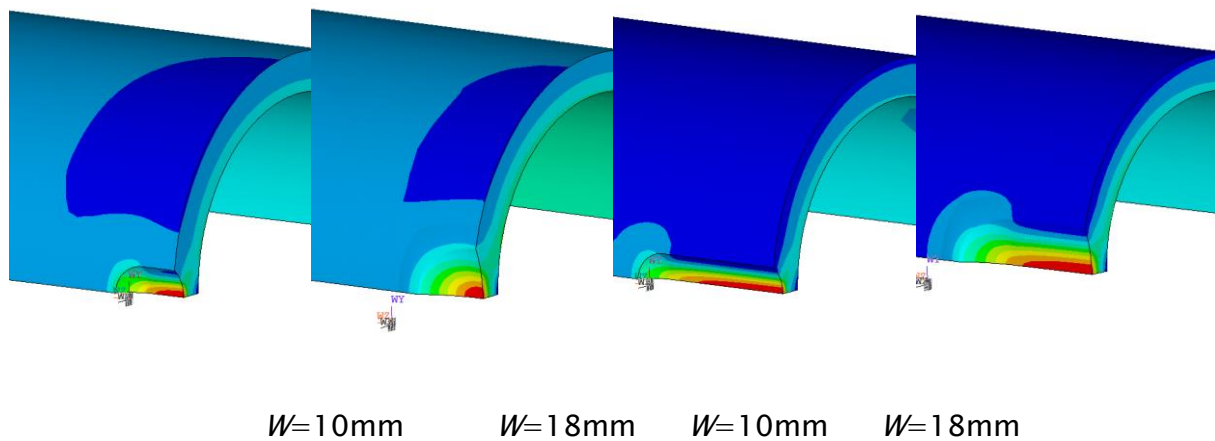


(a) The ellipsoidal pit defect



(b) The narrow and long defect

**Fig.10** Trends of the max von Mises stress with width of the defect



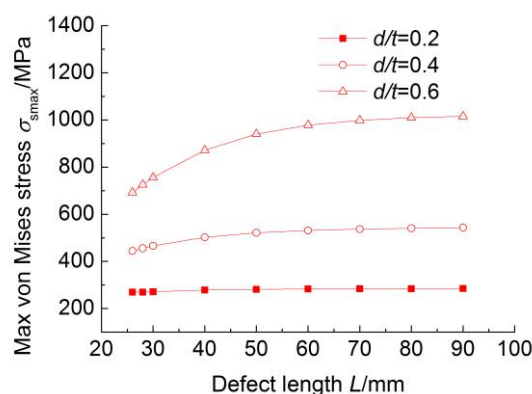
(a)The ellipsoidal pit defect

(b)The narrow and long defect

**Fig.11** The von Mises stress contours of defect areas with different defect width

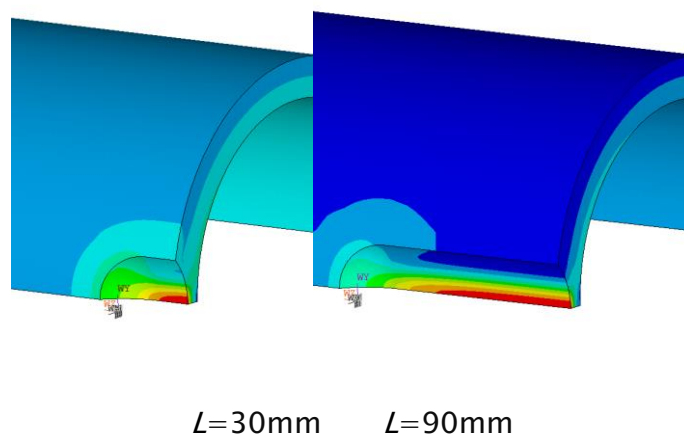
## Effects of defect length

Fig. 12 describes the influence of defect length  $L$  on the max von Mises stress in tube  $\sigma_{\text{max}}$ . Results show that, with the increase of defect length,  $\sigma_{\text{max}}$  increases. And with a larger defect depth, the increase rate is larger. Especially, when  $d/t=0.6$ ,  $\sigma_{\text{max}}$  increases with  $L$  obviously. When  $d/t=0.2$ ,  $\sigma_{\text{max}}$  varies a little with defect length increasing.



**Fig.12** Trends of the max von Mises stress with the length position of the defect

The von Mises stress contours for tubes with different defect lengths were shown in Fig. 13. For both conditions, the max von Mises stress concentrated in the circumferential central area of the defect. But with the increase of defect length, axial length of high stress area increases.



**Fig.13** The von Mises stress contours of defect areas with different defect length

## Residual strength prediction based on artificial neural network

In the previous section, parametric analysis was conducted by 264 cases with different combination of influence factors. Through this investigation, quantitative relationships between the max von Mises stress in tube with the influence factors were derived. In this section, a residual strength prediction model was proposed using BP artificial neural network.

## Basic procedure for BP ANN

BP artificial neural network (ANN) is a kind of multilayer perceptron, which is also known as feed forward multilayer neural network. It has three different layers, e.g. input layer, hidden layer and output layer. For hidden layer, it can be one layer or multi layers. Fig. 14 illustrate the algorithm of training procedure of BP ANN.

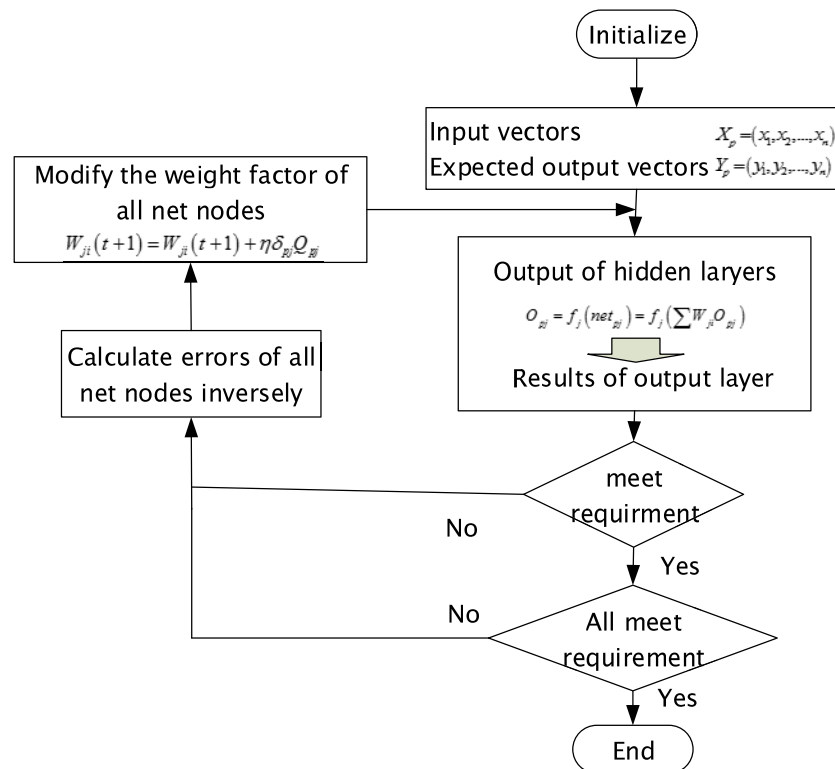


**Fig. 14** Training procedure for BP neural network

In this study, the neural network was established by the commercial software MATLAB, which has a neural network toolbox. The BP artificial neural network can be easily trained by the function 'trainlm' supported by MATLAB [17].

## Prediction model

From the parametric analysis, effect factors of residual strength of corroded oil tube can be concluded as defect location (Load condition), tube wall thickness, defect width, defect length, defect depth. Thus they are adopted as five input parameters in the input layer. And

the residual strength was set to be the output. In this model, the structure of the neural network was set as 5-11-1, as shown in Fig. 15.

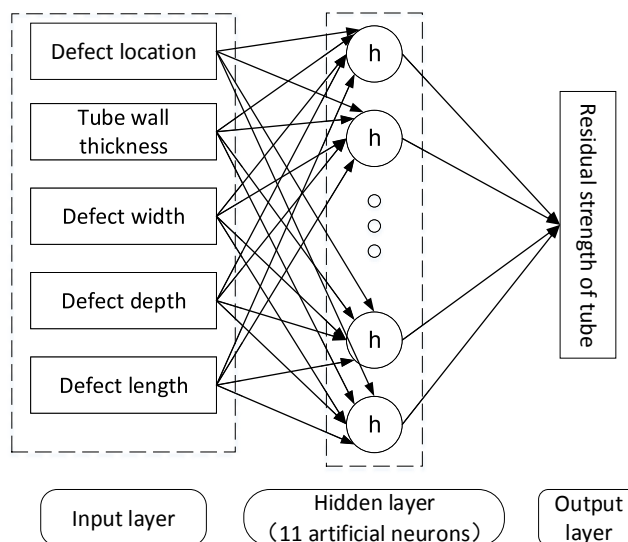


**Fig. 15** Neural network structure for limit pressure predicting of corroded pipes

264 case results were used to train the network. Fifteen percent of all cases were used as validation and another fifteen percent of all cases were used as test. The network training was completed at epoch 27 as shown in Fig. 16. The normalized results for the trained network was also illustrated in Fig. 17, which shows that the proposed model is accurate in residual strength prediction.

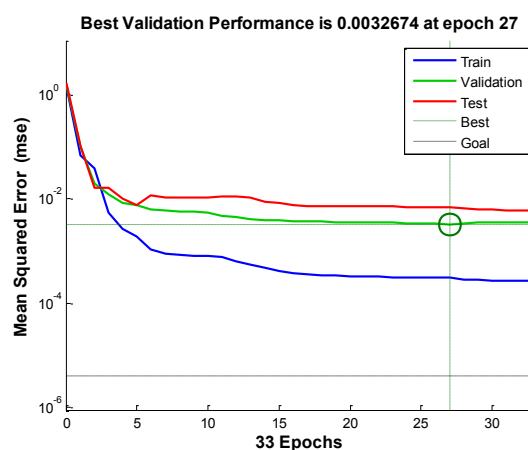


**Fig. 16** Training process of the BP artificial neural network



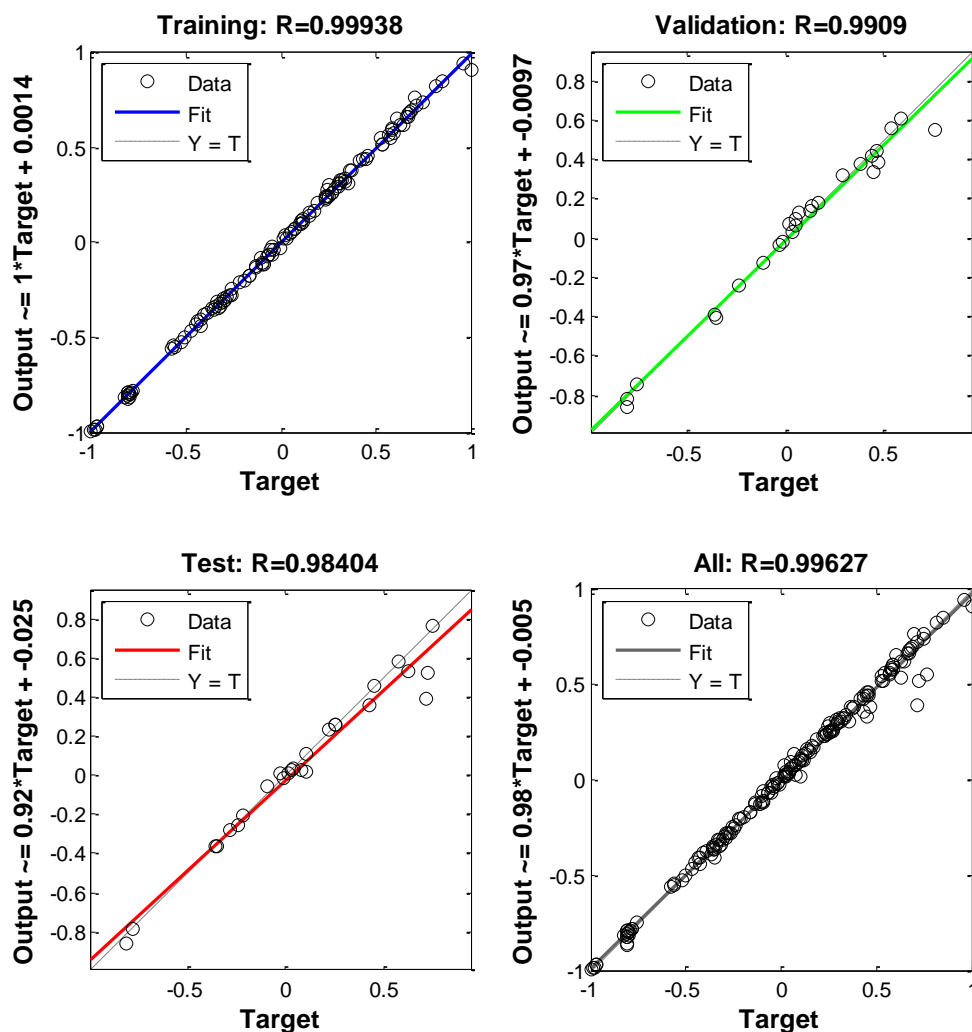


Fig. 17 Proposed BP neural network results

## Conclusion

Corssion is a main threat for oil tubes. In this paper, a refined numerical model for residual strength analysis of P110 oil tube with corrosion defects under serive load was established. Effects of common factors on tube's residual strength were derived by parametric analysis. What's more, a residual strength prediction model was propsod using BP artifical nueral networks. Some conclusions can be drawn:

- (1) The defect depth has more obvious effect on tube's strength comparing with the defect length and width. Thus, monitoring the depth of corrosion defects is more essential in engineering practice.
- (2) With increase of the depth of corrosion defect location in tube, the max von Mises stress in the tube decreases first and then increases for both ellipsoidal pit defect and narrow and long defect.
- (3) If location of the defect in tube is shallow, corrosion area may rupture in axial direction, and if location of the defect in tube is deep, corrosion area may rupture in circumferential direction.
- (4) The proposed residual strength prediction model is accurate for corroded P110 oil tube, which can be referenced in the safety assessment and equipment maintenance in oil field.

## Acknowledgements

The work was financially supported by China National Key Research and Development Project (Grant No. 2016YFC0802105). Science Foundation of China University of Petroleum, Beijing (Grant No. 2462015YQ0408, No. C201602 and No. 2462015YQ0403), National Natural Science Foundation of China (Grant No. 51309236), the Opening Fund of State Key Laboratory of Ocean Engineering (Shanghai Jiao Tong University) (Grant No. 1314), Opening Fund of State Key Laboratory of Hydraulic Engineering Simulation and Safety (Tianjin University) (Grant No. HESS-1411), Opening Fund of State Key Laboratory of Coastal and Offshore Engineering (Dalian University of Technology) (Grant No. LP1507).

## References

- [1] 'New methods for determining the remaining strength of corroded pipeline', A. Batte, B. Fu, M. Kirkwood, et al., *International Conference on Offshore Mechanics and Arctic Engineering*. OMAE. Yokohama, Japan, pp221–228, 1997.
- [2] 'Development of limit load solutions for corroded gas pipelines', J. Choi, B. Goo, J. Kim, et al. *International Journal of Pressure Vessels and Piping*, 80, pp121–128, 2003.
- [3] 'Limit load capacity of pipes with long longitudinal corrosion', Y. Chen, X. Li, J. Zhou, *Journal of Ship Mechanics*, 13, 5, pp748–756, 2009.

- [4] 'Prediction of failure pressure in corroded pipelines based on non-linear finite element analysis', J. Shuai, C. Zhang, F. Chen, *Acta Petrolei Sinica*, **29**, 6, pp933–937, 2008.
- [5] 'An alternative approach to assess the integrity of corroded line pipe–Part I: current status and Part II: alternative criterion', B. Leis, D. Stephens, *Proceedings of the 7th International Offshore and Polar Engineering Conference*, Honolulu, USA, May 25–30, 1997.
- [6] 'Development of an alternative criterion for residual strength of corrosion defects in moderate to high-toughness pipe', D. Stephens, B. Leis, *Proceedings of International Pipeline Conference*, Calgary, Alberta, Canada, September, pp10–13, 2000.
- [7] 'The effect of the width to length ratios of corrosion defects on the burst pressures of transmission pipelines', G. Fekete, L. Varga, *Engineering Failure Analysis*, **21**, pp21–30, 2012.
- [8] 'Study on failure assessment for X80 high-grade pipeline with corrosion defects', G. Xiao, M. Feng, H. Zhang, et al. *Journal of Safety Science and Technology*, **11**, 6, pp126–131, 2015.
- [9] 'Study on characteristics of safety assessment model on pipeline corrosion', S. Peng, H. Tang, Y. Ding, et al., *Journal of Safety Science and Technology*, **3**, pp172–178, 2015.
- [10] 'Study the waste standard of the defective oil pipe by finite element method', S. Zhou, D. He, Z. Lu, *Oil Field Equipment*, 2006, **35**, 6, pp19–22, 2006.
- [11] 'Reliability analysis of marine risers with narrow and long corrosion defects under combined loads', X. Hu, C. Zhou, M. Duan, et al. *Petroleum Science*, **11**:139–146, 2014.
- [12] 'Residual Strength Analysis of Oil Tubes with Corrosion Defect', M. Xia, Q. Duan, X. Liu et al., *Materials Science Forum*, 850:950–956, 2016.
- [13] 'Failure Analysis of Oil Tubes Containing Corrosion Defects Based on Finite Element Method', X. Liu, H. Zhang, et al., *International Journal of Electrochemical Science*, **11**, 5180–5196, 2016.
- [14] ISO/TR 10400, the International Organization for Standardization, 2007.
- [15] API Specification 5CT, Specification for Casing and Tubing, 2005.

- [16] 'A finite-element-based analysis of the accuracy in bursting tests predicting the ultimate load of a buried pipeline', B. Ma, J. Shuai, D. Liu, et al., *Natural Gas Industry*. **33**, 6, pp108–112, 2013.
- [17] 'Neural network toolbox for use with MATLAB. User's guide', D. Howard and B. Mark, 2006.